

# Mitigation of spectral mis-registration effects in imaging spectrometers via cubic spline interpolation

Yutao Feng<sup>1,2</sup>, Yang Xiang<sup>1,\*</sup>

<sup>1</sup>The State Key Laboratory of Applied Optics, Changchun Institute of Optics, Fine Mechanics and Physics, Jilin Changchun, 130033

<sup>2</sup>Graduate University of Chinese Academy of Sciences, Beijing, 100039

\*Corresponding author: [y.xiang@sklao.ac.cn](mailto:y.xiang@sklao.ac.cn)

**Abstract:** The effects of spectral curvature (smile) on the co-registration of measured radiance spectra were analyzed for a dispersive imaging spectrometer. The spectra measured by the imaging spectrometer with spectral curvature were re-sampled using cubic spline Interpolation to mitigate the mis-registration of spectral radiance measurement. After correction, the co-registration of measured radiance spectra is distinctly improved.

©2008 Optical Society of America

**OCIS Codes:** (010.4450) remote sensing, (110.4234) multispectral and hyperspectral imaging, spectral curvature (smile), (010.5630) spectral radiance measurement.

---

## References and links

- 1 R. O. Green, M. L. Eastwood, C. M. Sarture, T. G. Chrien, M. Aronsson, B. J. Chippendale, J. A. Faust, B. E. Pavri, C. J. Chovit, M. Solis, M. R. Olah, and O. Williams, "Imaging Spectroscopy and the Airborne Visible/Infrared Imaging Spectrometer (AVIRIS)," *Remote Sens. Environ.* **65**, 227–248 (1998).
- 2 R. O. Green, B. E. Pavri, and T. G. Chrien, "On-Orbit Radiometric and Spectral Calibration Characteristics of EO-1 Hyperion Derived With an Underflight of AVIRIS and In Situ Measurements at Salar de Arizaro, Argentina," *IEEE Trans. Geosci. Remote Sens.* **41**, 1194–1203 (2003).
- 3 L. Guanter, V. Estellés, and J. Moreno, "Spectral calibration and atmospheric correction of ultra-fine spectral and spatial resolution remote sensing data. Application to CASI-1500 data," *Remote Sens. Environ.* **109**, 54–65 (2007).
- 4 C. O. Davis, J. Bowles, R. A. Leathers, D. Korwan, T. V. Downes, W. A. Snyder, W. J. Rhea, and W. Chen, "Ocean PHILLS hyperspectral imager: design, characterization, and calibration," *Opt. Express* **10**, 210–221 (2002).
- 5 S. W. Brown, B. C. Johnson, S. F. Biggar, E. F. Zalewski, J. Cooper, P. Hajek, E. Hildum, P. Grant, R. A. Barnes, and J. J. Butler, "Radiometric validation of NASA's Ames Research Center's Sensor Calibration Laboratory," *Appl. Opt.* **44**, 6426–6444 (2005).
- 6 R. A. Barnes, R. E. Eplee, G. M. Schmidt, F. S. Patt, and C. R. McClain, "Calibration of SeaWiFS. I. Direct techniques," *Appl. Opt.* **40**, 6682–6690 (2001).
- 7 P. M. Teillet, G. Fedosejevs, R. P. Gauthiera, N. T. O'Neill, K. J. Thomec, S. F. Biggar, H. Ripleyd, and A. Meygrete, "A generalized approach to the vicarious calibration of multiple Earth observation sensors using hyperspectral data," *Remote Sens. Environ.* **77** 304–327 (2001).
- 8 R. O. Green, "Spectral calibration requirement for Earth-looking imaging spectrometers in the solar-reflected spectrum," *Appl. Opt.* **37**, 683–690 (1998).
- 9 J. J. Puschell, "Hyperspectral Imagers for Current and Future Missions," *Proc. SPIE* **4041**, 121–132. (2000)
- 10 F. Blechinger, B. Harnisch, and B. Kunkel. "Optical Concepts for High Resolution Imaging Spectrometers," *Proc. SPIE* **2480**, 165–179 (1995).
- 11 G. Recktenwald, *Numerical methods with Matlab implementation and application*, (China Machine Press, Beijing, 2004), 364–410.
- 12 B. C. Gao, M. J. Montesa, and C. O. Davis, "Refinement of wavelength calibrations of hyperspectral imaging data using a spectrum-matching technique," *Remote Sens. Environ.* **90**, 424–433 (2004).

## 1. Introduction

Imaging spectrometers measure spectrum of each spatial scene element in an image. It is necessary to keep the co-registration of the measured spectra for all scene elements. It is significant to analyze the effect of spectral offset on the measured radiance spectrum. The co-registration of the measured radiance spectra have been broadly studied during the process of spectral and radiometric calibration of each system, such as Airborne Visible/Infrared Imaging Spectrometer (AVIRIS), EO-1Hyperion, Compact Airborne Spectrographic Imager (CASI) and Ocean PHILLS hyperspectral imager [1-4]. There are certain spectral offsets on the pixels along cross-track array for each system, which destroy the co-registration of the measured radiance spectra. The radiometric calibration accuracy of an imaging spectrometer is commonly better than 5% [5-7]. Robert O. Green pointed out that a spectral uncertainty approaching 1% is necessary to suppress the errors in measured radiance spectrum [8]. A prism or grating is used to separate light for a Dispersive Imaging Spectrometer (DIS) [9]. There is spectral curvature (smile) on an image plane because of dispersion with non-main cross-section [10]. A spectral curvature brings the offset in the center wavelength and the spectral response function between the pixels in the same array but not column. Furthermore, spectral curvature reduces the co-registration of the measured radiance spectra. This analysis presents the errors in the measured radiance spectra brought by spectral curvature between the pixels in the same cross-track array. And the spectral radiance measured by the imaging spectrometer with spectral curvature was interpolated via Cubic Spline Interpolation (CSI) to mitigate the mis-registration of the measured radiance spectra.

## 2. The mis-registration of measured radiance spectra brought by spectral curvature

For a spaceborne pushbroom imaging spectrometer, the measured radiance  $\Phi_{i,j}$  of the detector pixel  $(i,j)$  is the convolution of the spectral response function  $f(\lambda-\lambda_{i,j})$  with a high-resolution spectrum  $L_i(\lambda)$  across the spectral band  $j$  [8]:

$$\Phi_{i,j} = A \int_{\lambda_{i,ja}}^{\lambda_{i,jb}} f(\lambda - \lambda_{i,j}) L_i(\lambda) d\lambda \quad (1)$$

Where:  $A$  is the systematic parameter of imaging spectrometer.  $\lambda_{i,j}$  is the center wavelength of spectral band  $j$  of the scene pixel  $i$ .  $\lambda_{i,ja}$  and  $\lambda_{i,jb}$  are the starting and cut-off wavelength of spectral band  $j$ .

If there were no spectral curvature, there would be the same center wavelength for all pixels in the same cross-track array  $j$  on the detector plane.  $\lambda_{i,j} = \lambda_j$ . While if there were spectral curvature on the detector plane, there would be certain center wavelength offset  $\delta_{m,j}$  of the pixel  $(i+m,j)$  relative to the pixel  $(i,j)$  (See Fig. 1),  $\lambda_{i+m,j} = \lambda_{i,j} + \delta_{m,j}$ . The integral range of Eq. (1) is also shifting  $\delta_{m,j}$ . So there will present mis-registration for spectral measurement along cross-track direction.

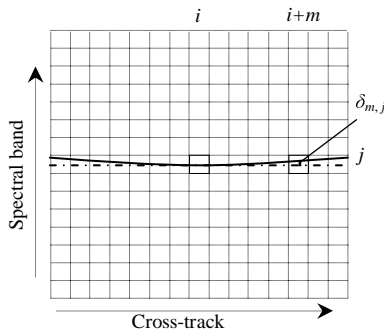


Fig. 1. Sketch map of spectral curvature (smile) on detector plane

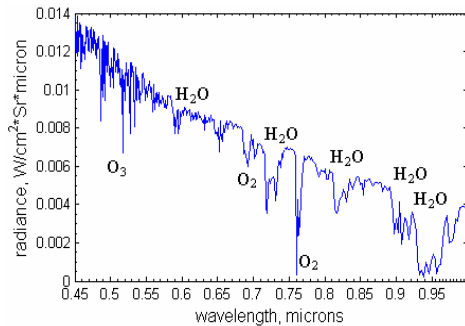


Fig. 2. Upwelling spectral radiance

In order to analyze the effects of spectral curvature (smile) on the co-registration of measured radiance spectra, it assumes that all ground source pixels have the same spectral radiance. An upwelling radiance spectrum at the top of the atmosphere was modeled in the range of 0.45~1.0 $\mu\text{m}$  with conditions of a 45° solar illumination angle, a 0.25 reflection horizontal surface at sea level, and the 23-km visibility standard mid-latitude summer atmosphere model (See Fig. 2) [3, 8]. For this analysis, the specified Gaussian function of a channel spectral response function  $f(\lambda-\lambda_{i,j})$  was evaluated for each wavelength of the high-resolution upwelling radiance spectrum. The spectral resolution of an imaging spectrometer is 5nm. In order to give prominence to the issue of mis-registration in spectral radiance measurement and its mitigation algorithm, the spectral curvature is assumed wavelength-independent. That makes calculation easy but dose not influence the validity and application. Using Eq. (1), the radiance spectra measured by each detector pixels in the columns  $i$  and  $i+m$  were calculated respectively. The relative percent error in measured radiance between the detector pixels  $(i+m, j)$  and  $(i, j)$  on can be express as

$$\Delta\Phi_{m,j} = \frac{\Phi_{i+m,j} - \Phi_{i,j}}{\Phi_{i,j}} \times 100\% \quad (2)$$

Equation (2) shows the mis-registration of measured spectral radiance in the spectral band  $j$  between the source pixels  $i$  and  $i+m$ . if there were no spectral curvature on image plane,  $\Phi_{i+m,j}$  would be equal to  $\Phi_{i,j}$ ,  $\Delta\Phi_{m,j}=0$ . Figure 3 shows the relative percent error in the measured radiance spectra between two source pixels  $i$  and  $i+m$  in the same cross-track array. Near the O<sub>2</sub> absorption at 0.76 $\mu\text{m}$  and the atmosphere water-vapor absorption at 940 $\mu\text{m}$ , the measured radiance presents distinct errors. The errors in the measured radiance strongly depend on the spectral offset  $\delta_{m,j}$  between the pixels in column  $i+m$  and  $i$  on the detector plane. In Fig. 3a, an offset of  $\delta_{m,j}=1\%\Delta\lambda$  ( $\Delta\lambda$  is spectral channel increment) for the pixels in the column  $i+m$  relative to the pixels in the column  $i$  results in the maximum  $\pm 2\%$  error, the errors in measured radiance is very small. The mis-registration of measured radiance spectra can be neglected. But in Fig. 3(b), an offset of  $\delta_{m,j}=10\%\Delta\lambda$  for the pixels in the column  $i+m$  relative to column  $i$  results in the maximum  $\pm 15\%$  error. The errors in measured radiance are larger in errors of  $30\%\Delta\lambda$  or  $50\%\Delta\lambda$ . The mis-registration of measured radiance spectrum is much serious, it needs to be corrected.

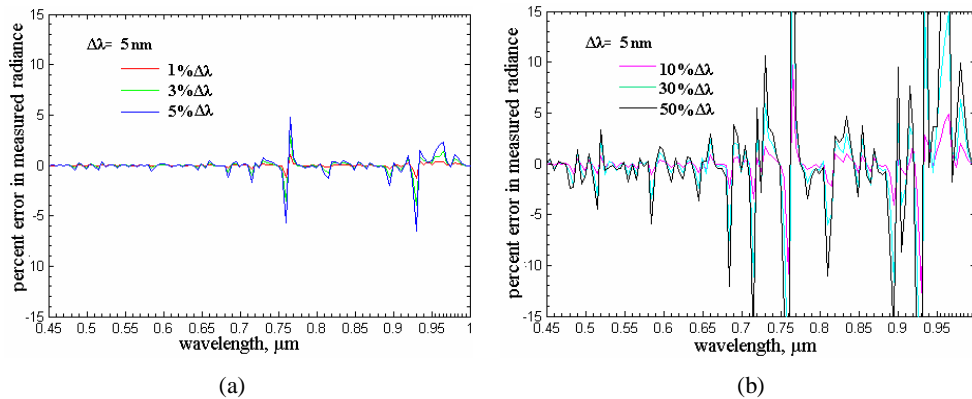


Fig. 3. Percent error in measured radiance for an imaging spectrometer with spectral curvature resulting from (a) spectral offset 1% $\Delta\lambda$ , 3% $\Delta\lambda$ , 5% $\Delta\lambda$  and (b) spectral offset 10% $\Delta\lambda$ , 30% $\Delta\lambda$ , 50% $\Delta\lambda$

### 3. Correction

In order to mitigate the mis-registration of measured radiance spectra, the spectral radiance

measured by the detector pixels in the column  $i+m$  was re-sampled to acquire the approximations of the measured radiance corresponding to the center wavelengths of the detector pixels in the column  $i$ . The common interpolation methods are Linear Interpolation (LI), Cubic Hermite Interpolation (CHI), Cubic Spline Interpolation (CSI) and so on [11]. Because the measured spectral radiances are varying strongly with respect to wavelength by the atmosphere and solar absorptions throughout the whole spectral range, it is necessary to choose a correct interpolation method. The comparisons of the capabilities of above-mentioned method are shown in Fig. 4. For the purpose of contrast, Fig. 4a shows the percent errors in measured spectral radiance with  $10\% \Delta\lambda$  spectral offset before correction. Figure 4(b) shows the percent errors in the measured spectral radiance that corrected with each interpolation method. It is obvious that using CSI to correct the errors in the measured radiance is much better than other two methods. The residual errors with CSI are small than that with LI and CHI in full spectral range. Especially, using LI method sometimes makes residual errors larger than that un-corrected at some wavelength, such as the red line close to  $0.94\mu\text{m}$ . The LI using first-order piecewise polynomial cannot make the curve well smooth. The CHI needs the interpolating function and its first derivative keeping continuous at piecewise nodes. The CSI needs the interpolating function and its first and second derivative keeping continuous at piecewise nodes [11]. So the CSI is chose to mitigate the mis-registration of spectral radiance measured by an imaging spectrometer with spectral curvature.

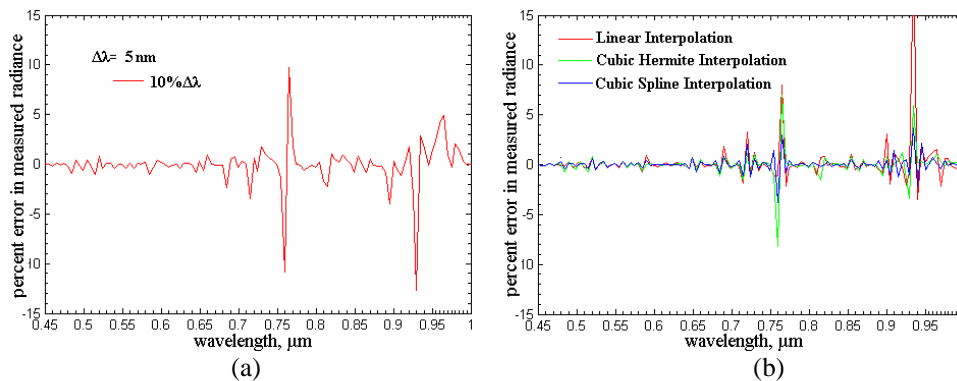


Fig. 4. Comparisons of three interpolation methods. (a) shows the percent errors in measured spectral radiance with  $10\% \Delta\lambda$  spectral offset. (b) shows residual errors in the measured radiance corrected with each interpolation method.

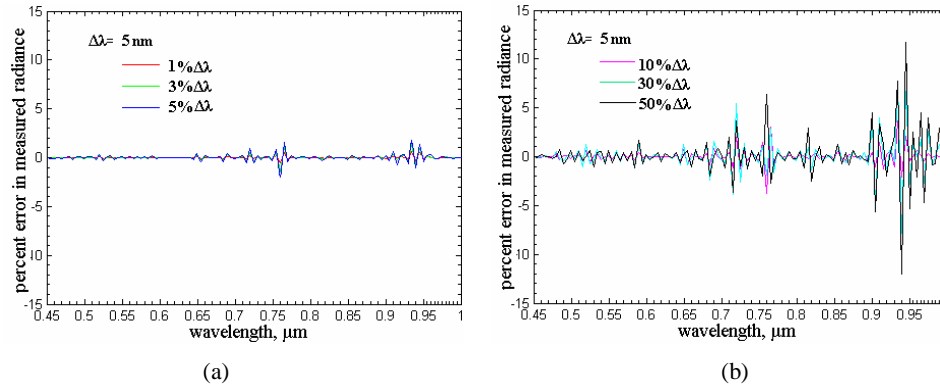


Fig. 5. The residual error in measured radiance after corrected by CSI. (a) spectral offset  $1\% \Delta\lambda$ ,  $3\% \Delta\lambda$ ,  $5\% \Delta\lambda$  and (b) spectral offset  $10\% \Delta\lambda$ ,  $30\% \Delta\lambda$ ,  $50\% \Delta\lambda$ .

The percent errors in the corrected measured radiance are shown in Fig. 5. Compared with Fig. 3, the positions that correspond to the distinct errors in the measured radiance are not change, but the magnitudes of the errors are averagely reduced 60%. In Fig. 5(b), for an spectral offset  $\delta_{m,j}=50\% \Delta\lambda$ , the residual error in the corrected measured radiance is less than 15%. When the spectral offset is smaller than  $5\% \Delta\lambda$ , the errors in measured radiance can be suppressed well by re-sampling with CSI (see Fig. 5(a)). The mis-registration of spectral radiance measurement can be neglected.

#### 4 Discussions

The spectral radiance measured by dispersive imaging spectrometers spans a range of atmosphere, ground scene and observation conditions. For this analysis a single modeled high-resolution radiance spectrum and a simple model of systematic spectral curvature were used. Nevertheless, the mis-registration of the measured radiance spectra with spectral curvature and its mitigation algorithm discussed in this paper are generally applicable. There are three reasons. Firstly, the distinct errors in co-registration of the measured radiance spectra are all present at the atmosphere and solar absorptions. The strengths of the atmosphere absorptions vary with atmosphere composition and observation conditions, but the absorptions are always present and their positions are invariable. A uniform ground scene spectrum was used with a 0.25 reflection, but a true scene reflection spectrum just adds the distinct radiance errors in the regions of the scene absorptions. Secondly, using relative percent errors in the measured radiance to denote the mis-registration of spectral radiance measurement makes the results independent of the instrumental parameter  $A$ . the results are dependent on the offset in center wavelength and the FWHM of spectral response function that determines the convolution of the narrow spectral bands of the imaging spectrometer with the upwelling spectral radiance. Finally, the spectral curvature is a wavelength-dependent effect. In practice, the offsets in center wavelength and FWHM across the spectral bands in the same column can be calculated according to the dispersive properties of an imaging spectrometer. The measured radiance is the convolution of different spectral response function of each spectral band with the upwelling spectral radiance that contains narrow atmosphere and scene absorptions. The spectral offset in certain column with fix value in this analysis just makes the calculation easy. The issue and method discussed in this paper are generally applicable.

For an observed area with the upwelling spectral radiance shown in Fig. 6 (modeled with grassland and subarctic winter atmosphere model), the percent errors in the measured radiance spectra between two cross-track source pixels  $i$  and  $i+m$  are shown in Fig. 8 with  $5\% \Delta\lambda$  and  $10\% \Delta\lambda$  spectral offsets. The upwelling spectral radiance shown in Fig. 6 is much different

from that in Fig. 2 and the strengths of the atmosphere absorptions are weaker especially water-vapor absorptions, but the positions that correspond to the distinct errors in the measured radiance are still unchanged for Fig. 7 compared with Fig. 3. There are some new positions that correspond to the small errors present in Fig. 7(a). Because the spectral bands with  $\Delta\lambda=2.5\text{nm}$  narrower than  $\Delta\lambda=5\text{nm}$  would continue to be sensitive to the increasingly fine atmosphere and scene absorptions contained in upwelling spectral radiance. In Fig. 7(b), Apparently, the errors are just present at the strong atmosphere  $\text{O}_2$  and water-vapor absorptions because the wider spectral bands  $\Delta\lambda=10\text{nm}$  become less sensitive to the fine atmosphere absorptions. Figure 8 shows the corrected percent errors in measured radiance corresponding to Fig. 7. The positions that correspond to the distinct errors in the measured radiance spectra are not change, but the magnitudes of the errors are averagely reduced at least 60%. Especially, the mis-registration of the spectral radiance measurement is corrected well in Fig. 8(a). Because with narrow spectral bands  $\Delta\lambda=2.5$  there are more data to be used to interpolate. When the spectral offsets are no more than  $5\%\Delta\lambda$ , the mis-registration of the spectral radiance measurement can be mitigated well via cubic spline interpolation. The residual percent errors are no more than 2% for  $\Delta\lambda=2.5\text{nm}$ ,  $5\text{nm}$  and  $10\text{nm}$ .

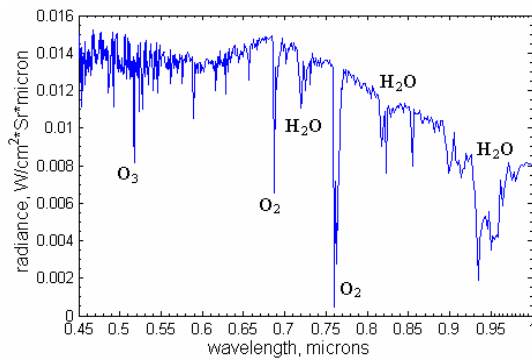


Fig. 6. The upwelling spectral radiance modeled with grassland and subarctic winter atmosphere model.

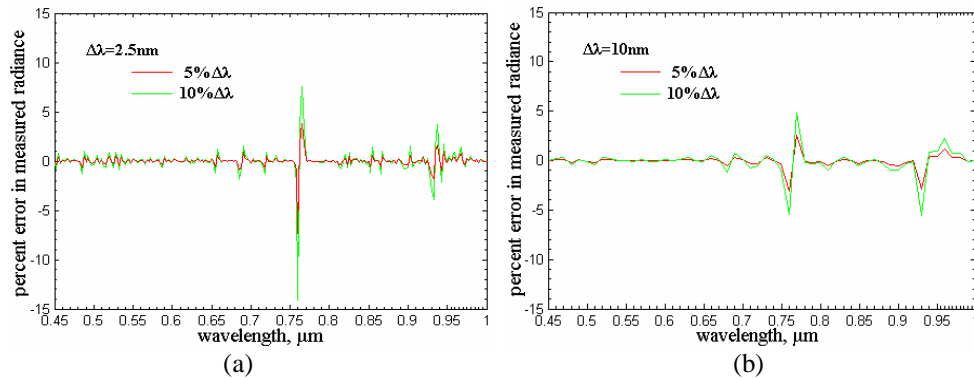


Fig. 7. Percent error in measured radiance for spectral offsets  $5\%\Delta\lambda$  and  $10\%\Delta\lambda$ , (a) spectral resolution  $\Delta\lambda=2.5\text{nm}$  and (a) spectral resolution  $\Delta\lambda=10\text{nm}$ .

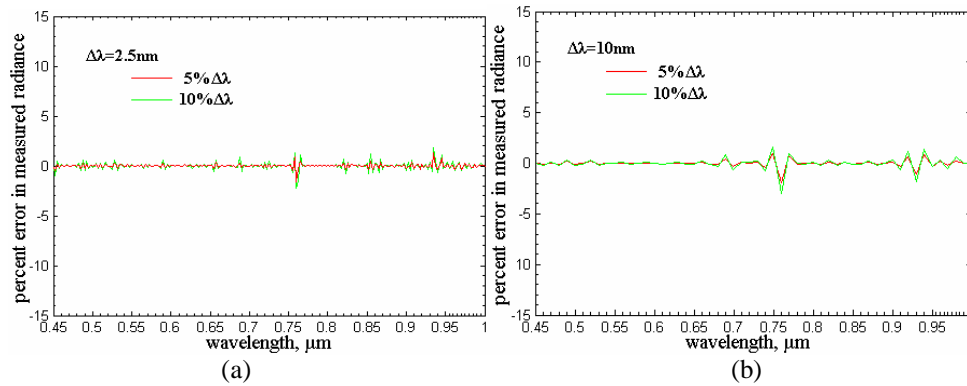


Fig. 8. Percent error in corrected measured radiance for spectral offsets  $5\% \Delta\lambda$  and  $10\% \Delta\lambda$ , (a) spectral resolution  $\Delta\lambda=2.5\text{nm}$  and (a) spectral resolution  $\Delta\lambda=10\text{nm}$ .

Besides the spectrum of the observed scene, the scene image corresponding to a center wavelength of spectral band can be obtained from the spectral data cube measured by an imaging spectrometer. Spectral curvature destroys the co-registration of spectral radiance measurement. It is inevitable to affect the scene image. Figure 9 shows the gray-scale images of a ground area corresponding to  $0.765\mu\text{m}$  (a) and  $0.93\mu\text{m}$  (b) spectral bands. The ground scene and atmosphere conditions are the same as that mentioned in section 2. Assume that the maximum spectral offset  $\delta_{512,j}$  is  $50\% \Delta\lambda$  ( $\Delta\lambda=5\text{nm}$ ). All measured radiance data are normalized by the maximum of them measured by imaging spectrometer without spectral curvature. Figure 9(a) is the gray-scale images of ground scene measured without spectral curvature. According to the assumption, all ground scene pixels ( $512 \times 512$ ) have the same spectra. So the gray-scale images corresponding to  $0.765\mu\text{m}$  (a) and  $0.93\mu\text{m}$  (b) spectral bands are two planes with fixed gray level. When there are spectral offsets on the detector derived from spectral curvature, the gray-scale images of two spectral bands are not planes with fixed gray level any longer (see Fig. 9(b)). The differences of gray level between the cross-track pixels (0~512) become larger with the spectral offsets increasing. The imaging spectrometer with spectral curvature would obtain different gray-scale images corresponding to a certain spectral band for the same observed scene at different cross-track positions. For actual application, It is required that the instruments have the same response to the same observed scene no matter where the scene is along cross-track positions. Using CSI to mitigate the mis-registration of the spectral radiance measurement can also improve the uniformity of the gray-scale image of certain spectral band for the observed scene at different cross-track positions. Fig. 9C shows the gray-scale images corresponding to  $0.765\mu\text{m}$  (a) and  $0.93\mu\text{m}$  (b) spectral bands that the mis-registration of spectral radiance measurement has been mitigated via cubic spline interpolation. The images corresponding to  $0.93\mu\text{m}$  (b) in Figs. 9(c) and 9(a) are nearly same. The image corresponding to  $0.765\mu\text{m}$  (b) in Fig. 9(c) is more uniform than that in Fig. 9(b).

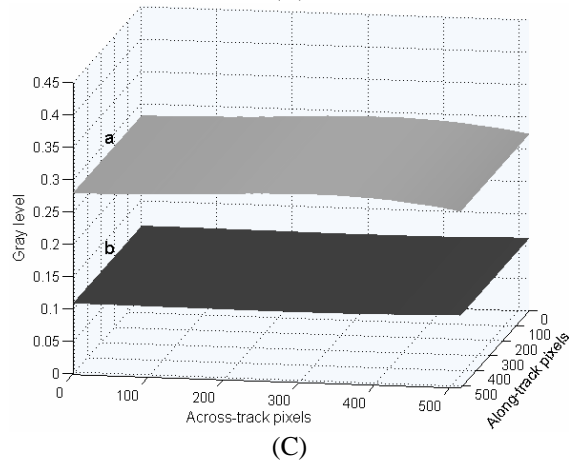
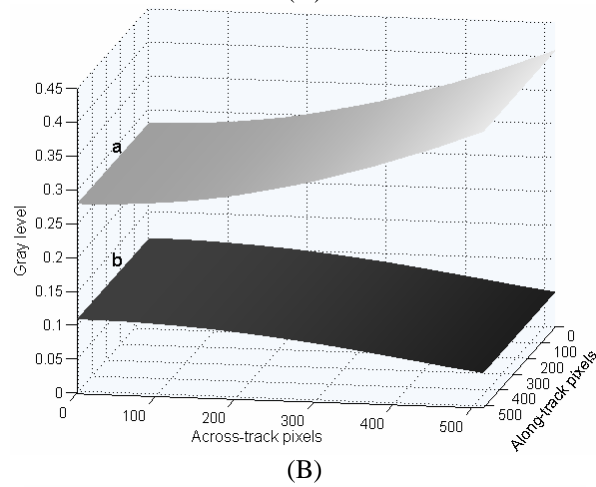
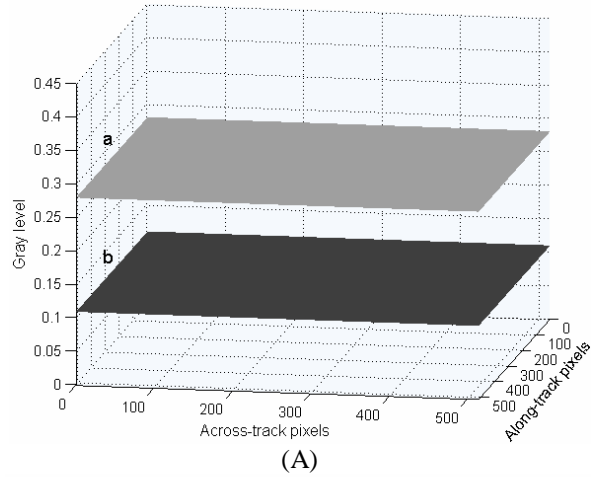


Fig. 9. The gray-scale images of a ground area corresponding to (a)  $0.765\mu\text{m}$  and (b)  $0.93\mu\text{m}$  spectral bands. (a) Without spectral offset. (b) With spectral offset. (c) After correction.

The spectral curvature is the intrinsic property of dispersive imaging spectrometer. It can be compensated during the process of optical design of the instrument. But the imaging



quality would become bad. In order to keep a high imaging quality, some spectral curvature would not be corrected by design. So the spectral offsets derived from residual spectral curvature will present on the detector plane of dispersive imaging spectrometer. In addition, the spectral offsets on the detector plane may occur when an imaging spectrometer is airborne or spaceborne due to vibrations, and to changes in instrument temperature and pressure [12]. Spectral offsets on the detector plane destroy the co-registration of spectral radiance measurement and bring errors in the spectral image. Fortunately, the values of spectral offsets can be determined according to the optical design parameters of the instrument or using the algorithm based on spectrum matching of certain atmosphere absorption from the data obtained by imaging spectrometer [12]. So the center wavelength with offsets can be determined. And then the measured radiance spectra with spectral offsets are re-sampled via cubic spline interpolation to obtain the approximations of the measured radiance corresponding to the original calibrated center wavelengths of spectral bands. Cubic spline interpolation can effectively correct the errors in the measured radiance and mitigate the mis-registration of spectral radiance measurement.

## 5. Conclusions

For a dispersive imaging spectrometer, spectral curvature destroys the co-registration of spectral radiance measurement and brings errors in measured radiance. Cubic spline interpolation can effectively correct the errors in the measured radiance and mitigate the mis-registration of spectral radiance measurement. The magnitudes of the errors in the measured radiance are averagely reduced at least 60%. When the spectral offsets are no more than  $5\% \Delta\lambda$ , the mis-registration of the spectral radiance measurement can be mitigated well via cubic spline interpolation for previous high resolution imaging spectrometer with spectral resolution about 5nm or 10nm. The residual percent errors are no more than 2%. This can loosen the requirement on spectral calibration accuracy and optical design parameters. This approach can be applied in other spectral ranges or other spectral offset brought by system vibration to improve the co-registration of the measured radiance spectra.

## Acknowledgments

This research was granted by the National Science Foundation of China (Grant No.:60538020) and CAS Innovation Program.